

Analysis of effect of impeller geometry including blade outlet angle on the performance of multi-pressure pumps: Simulation and experiment

N. Mohammadi*, **M. Fakharzadeh****

**Department of Mechanical Engineering, Islamic Azad University, Parand Branch, Parand, Iran,*

E-mail: nmohamady@ut.ac.ir

***Department of Mechanical Engineering, Islamic Azad University, Parand Branch, Parand, Iran,*

E-mail: fakharzadeh.mahdi@yahoo.com

crossref <http://dx.doi.org/10.5755/j01.mech.23.1.17676>

1. Introduction

Today, using pumps, to increase the liquid flow power, plays an important role in economic arenas as well as energy generation and water working projects. Centrifugal pumps have found increased applications in different industries where they have served as heart of a system to displace some fluid(s); these pumps, however, consume a large portion of total energy consumed by such systems. Centrifugal pumps have been widely applied across different industries including petrochemical complexes, refineries, thermal power plants, military industries, nuclear plants, agriculture and visually every industry where there may be a need for increased fluid flow pressure. As such, many researchers have tried to improve the performance of such pumps.

One of the principle parameters to consider when choosing a pump is the generable head by the pump which is a function of different parameters such as impeller diameter, pump rotational speed, pump flow rate, blade output angle, and the number of blades [1]. One-dimensional Euler's theory is usually utilized when designing the pumps. In order to ensure one-dimensionality of the flow, infinite number of blades is assumed with zero thickness; an ideal assumption which is obviously impossible to reach in reality. As the number of blades reduces, the flow loses its one-dimensionality within the area between the blades and may no more conform from the vane; this may reduce the pump head to a lower head than that of Euler [2, 3].

In order to increase pump head and efficiency, rather than arranging the pumps in series or parallel configurations, one can use a multi-stage or multi-pressure pump which principally works on a similar basis to that of centrifugal pumps. A multi-stage pump enjoys impellers of the same size which are designed for the same capacity. A two-stage pump, for example, performs much like two single-stage ones arranged in series. The first pump's output is fed into the second pump to further increase the head at the second impeller's output. With increasing the number of impellers increases, one may expect the ultimate output head to rise. One of the issues arisen when using multi-stage pumps is the cavitation phenomenon. This phenomenon may contribute into performance losses of the pump, corrosion of the blades and the shell, increased noises and unwanted vibrations of the pump. Prior to use the pump, in order to prevent potential damages to the pump, one should forecast the behavior of the flow inside the pump. For this purpose, before actually operating the pump, ANSYS Fluent software is utilized to expose the

pump to three-dimensional complex flows and turbulences. It is very expensive, time-intensive and boring to try to analyze the flow through the experimentations and model tests. As such, Computational Fluid Dynamics (CFD) is usually used to have the fluid flow analyzed. In the recent years, many industries have used this knowledge, as a powerful numerical simulation tool, to analyze fluid flows and centrifugal pumps.

Zhou [4] simulated the internal flow within three types of centrifugal pumps with 4 straight blades and 12 twisted ones, in two scales. In his research, he employed a commercial three-dimensional Navier-Stokes code, called CFX, using a $k-\epsilon$ standard turbulence model. Also, he used triangular grids to mesh the hub, mid span, and shroud before introducing the meshed impellers into the CFX environment. Furthermore, pressure and velocity distribution vectors corresponding to different periods were obtained for all the three impellers. The research results proved that one can enhance the pump efficiency using curved blades rather than straight ones.

Bross et al. [5] used experimental approaches along with numerical CFD-based methods to determine streamlines within the shroud, hub, and on the blades of an impeller. They investigated the effect of Reynolds number on the outlet flow angle. They further calculated the values of velocity and pressure across different zones around the impellers of the pumps.

Thin Cho Thin [6] analyzed the passing flow through a single-stage, single-suction pump. He showed that different losses may affect the corresponding performance curve to the pump. Hydraulic losses (due to friction, changes in flow direction, or changes in the cross section area of the volute casing) developed along the fluid flow path impose significant effect on the pump flow rate, head and power consumption. This impact may lead to increased power consumption yet reduced the pump head. He further illustrated that, one can rise the pump's output head by controlling and reducing the impeller friction losses, shock losses, disc friction losses, volute friction losses, and recirculation losses. He discussed the advantageousness of the centrifugal pumps, over other sorts of pumps, in terms of such characteristics as higher efficiencies, continuous flow and easier installation and maintenance protocols.

Anagnostopoulos [7] evaluated pumps performances in terms of efficiency. Estimating total hydraulic losses incurred across a pump's internal and external parts as well as its casing, he used, with the help of evaluation software, an optimized numerical algorithm based on unconstrained gradient to determine the pump's maximum

efficiency. Aiming at better fitness of the meshing elements at irregular boundaries, so as to achieve results of higher accuracy, he used advanced numerical techniques. He showed that hydraulic losses within volute casing and also in the pump inlet and outlet may contribute into reduced pump head.

Asilios [8] demonstrated that the geometry of a blade's leading edge may play an important role in the design of the blade. He performed a set of tests on a 9-blade impeller. A number of points at the blade tip were considered as control points with the effects of changes and displacements of these points on the pump power consumption and head been demonstrated. He used averaged Navier-Stokes equations using a $k-\epsilon$ standard turbulence model with control volume approach to optimize the internal geometry of the blades of the impeller in the centrifugal pump.

Kergourlay et al. [9] investigated the effects of splitters in the design of turbo-machines. In a centrifugal pump, too many or too few number of blades may result in the interference of the flows inside the impeller. It is expected that, head and efficiency increase with increasing the number of blades; however, such factors as the intensification phenomenon, blockage phenomenon due to blade thickness, and also increased friction along the guide vane contribute to efficiency losses. On the other hand, for a case where the number of blades is not adequate, the fluid may not follow one-dimensional flow principles within the impeller with local losses (leakage) increased. Therefore, one can see that pump performance is affected by the increases in hydraulic losses. Hydraulic losses can be reduced using splitters. These blades (splitters) are mounted on the central axis of the main blades to enhance absolute velocity and total pressure.

Changing the geometry of impeller's blades of a centrifugal pump, Bacharoudis et al. [10] investigated the pump performance. Their results indicated a good correlation between local and global parameters. Using a finite volume CFD program, the research provided a numerical solution for three-dimensional incompressible Navier-Stokes equations in an irregular grid system. Furthermore, flow pattern and pressure distribution along the guide vanes were calculated and flow rate-head curves were compared and discussed.

Houlin et al. [11] investigated the contributions from the number of blades into the specifications of a centrifugal pump. Flow analyses showed that, changes in the number of blades imposes very large effects not only on the low-pressure zones behind the internal blade, but also on the jet-wave structure in impellers. With increasing the number of blades, one can expect the pump head to increase as well. In this research, optimum number of blades to achieve the maximum pump efficiency is calculated. Furthermore, optimum number of blades to minimize the cavitation phenomenon is calculated.

Tverdokhleba [12] proposed the use of multi-stage pumps, rather than large-radius pumps, when a high level of output energy was demanded. He evaluated the products of HMS Company and used Ansys CFX to model fluid flow, velocity distribution, and pressure distribution across internal volumes. He demonstrated that using two-row pumps, one can attenuate the amplitude of pressure pulsations and enhance vibration characteristics.

Using tests and LDV measurements along with CFD techniques, Wen-Guang [13] determined fluid (water and oil) velocity in the impeller as well as volute casing of a centrifugal pump. He proved the slip factor to be a very important factor when hydraulically designing impellers of centrifugal pumps intended to work with oil. In this research, the effect of fluid type (water and oil) was evaluated on the pump output head and flow rate. He showed that the type of fluid within the impeller may directly contribute to the pump head and efficiency and shaft power.

Based on genetic algorithm optimization approach, Yang Sun-Sheng [14] undertook hydraulic design of an impeller for a centrifugal pump. He compared six impellers of single-arc, double-arc and triple-arc, logarithmic spiral and variable angle spiral to investigate the effect of impeller trimming on the pump performance. The optimization results revealed that the resulting impeller exhibited better performance in terms of efficiency and required torque to run the impeller. Also in this research, numerical results were compared to experimental data.

Using three-dimensional Navier-Stokes equations, Bellary et al. [15] optimized the shape of blades on the impeller of a centrifugal pump. They incorporated CFD into press based averaging method. In their research, the head, efficiency, and power consumption versus flow rate curves for three fluids: water, oil, gasoil were obtained. They showed that the effect of flow loss across the impeller's shroud and hub may contribute increased efficiency. Further, the effect of outlet and inlet angles on the efficiency was considered and showed that, compared to inlet angle; the outlet angle may have much larger contribution into pump efficiency.

Qing Zhang et al. [16] used CFD to investigate the effect of impeller inlet width of a centrifugal pump on its head and efficiency levels. For different values of impeller inlet width, they developed pressure distribution contours across various zones. The results indicated the maximum pump efficiency and head to correspond to an inlet width of 66 mm.

In the present research, using experimentations as well as numerical simulations, the effect of the blade geometry (including blade outlet angle) of a multi-pressure pump on the pump head and efficiency is studied. At specific values of outlet angle and blade width, hydraulic and mechanical losses within the impeller are reduced along with increases in the pump head and efficiency. Simulation results exhibit very good agreement with experimental data; Therefore, using numerical simulations with the help of ANSYS Fluent (rather than conducting actual tests), one can save both time and money.

2. Numerical simulation

Analyzed here is a closed single-suction, five-blade impeller with hub and shroud coverings (see Fig. 1). Impeller model was generated in SOLIDWORKS software before analyzing the fluid flow using ANSYS Fluent software. In order to compare simulation results to those of experiments and validate the numerical solution, model parameters and values were set to correspond to test conditions. Characteristics of the impeller are reported in Table 1.

Impeller characteristics

Outlet angle, Degree	Inlet angle, Degree	Inlet width, mm	Outlet width, mm	Thickness, mm	Outer diameter D_o , mm	Inner diameter D_I , mm	Number of Blade
27, 30 and 33	18	42	13	4	304	125	5



Fig. 1 Pump impeller

2.1. Meshing

Cartesian grid system is used in this research.

This meshing approach is preferred over other meshing techniques in terms of the fastness and accuracy. Development of an adequate grid system represents the most basic yet important step to undertake in the course of solving a problem via CFD-based approaches. Meshing plays an important role in the convergence, required time to achieve and the resulting accuracy of the problem solution. Multi-block meshing method was used here. In order to further enhance the fastness of the calculations and meshing task, the impeller was divided into five even sections (sectors) among which one sector was analyzed (see Fig. 2). Each sector was split into two zones. The first zone encompasses the space around and in-between the pump blades (moving zone), while the second zone encompasses the remaining portion of the sector (stationary zone). In order to provide adequate grids to boundary layer areas surrounding the blades, moving zone, and the areas near the blades, the grids within these areas should be set to be as small as possible.

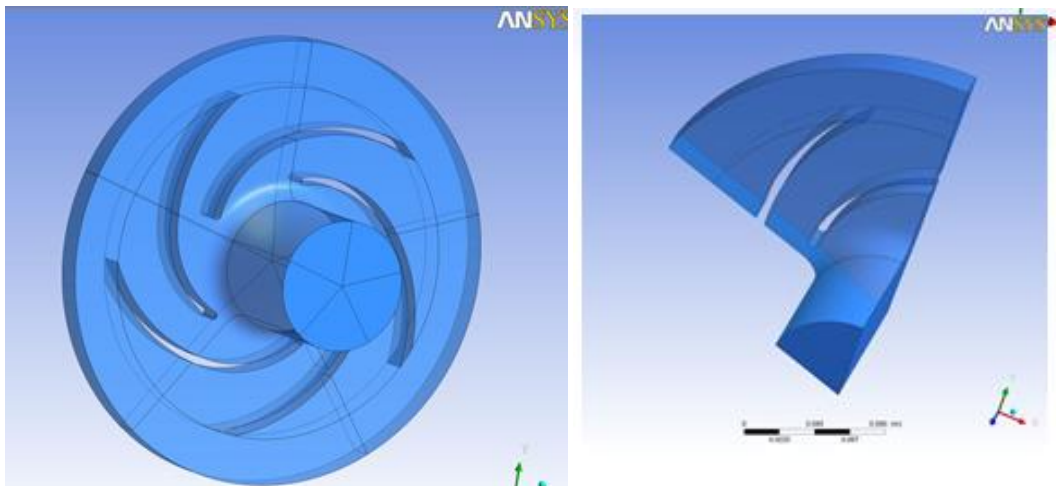


Fig. 2 Division of the impeller into five zones

2.2. Surface meshing

Since unstructured meshing approach have been already shown to be well-suited, unconstrained to mesh surfaces of the objects of complex geometries, this meshing approach was undertaken for all surfaces in this research. Higher speeds and lower boundary layer thicknesses observed close to the blade tip implied that smaller grids should be used across these areas, so as to consider the effects of boundary layer. Blade surfaces were meshed with squared elements. In order to properly model the boundary layer and tip vortexes, the size of the square sides were set to $0.001 D_o$ for the blade edges, blade tip, and areas close to the root. Other surfaces were meshed with larger square cells of approximately $0.01 D_o$ side lengths.

2.3. Volume meshing

In order to have volumes meshed, unstructured meshing approach was implemented via the TGrid algorithm. The generated elements by this algorithm were quadtrial of specific sizes. This algorithm allows some secondary elements to be generated with different sizes than those of the primary ones. In general, in volumetric meshing, aspect ratio parameter may not exceed 0.95, because failure to meet this criterion may lag the convergence to the solution or even make the solution diverged. As such, it is recommended to keep this parameter below 0.8 with its ideal value being 0.5. Here, the maximum allowable value of this parameter was set to 0.6. In addition, it is better for each element to have a size not greater than 1.2 times the size of the adjacent element. Fig. 3 illustrates the meshing approach for moving zone and around the blades.

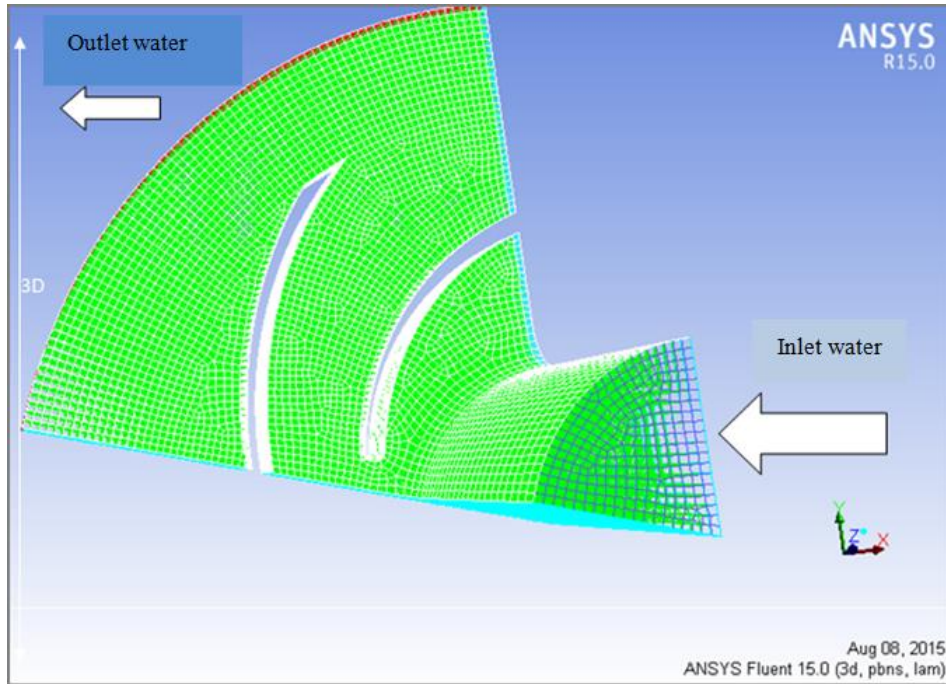


Fig. 3 Impeller meshing

2.4. Boundary conditions

The fluid pressure at the fluid inlet of the control volume (inlet extension) and also at the fluid outlet of the

control volume (outlet extension) was considered as the boundary conditions. The $k-\epsilon$ use as the turbulence model in the simulation. Fig. 4 presents inlet pressure and outlet pressure boundary conditions.

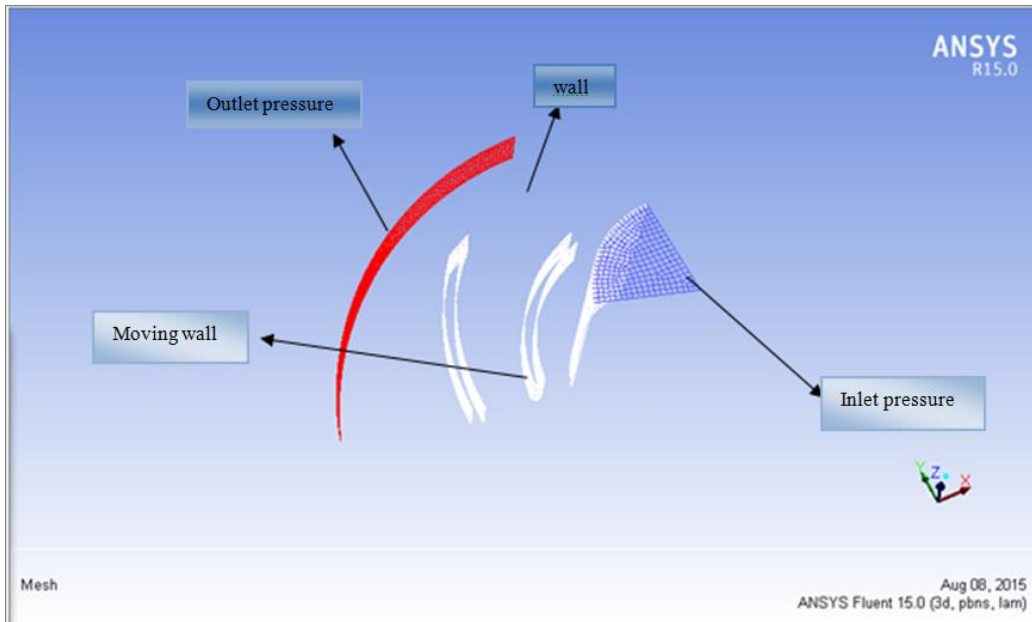


Fig. 4 Pressure boundary conditions

3. Numerical results

First, pressure distribution contours were plotted for different flow velocities (flow rates) across different zones on the impeller. In this phase, pressure distribution contours, pump head and efficiency values were obtained at eight different flow rates. Using Eq. (1), pump flow rate was determined at different flow velocities. Also, with the help of Eq. (2), total pressure contours were used to obtain the pump head values.

$$Q = VA ; \quad (1)$$

$$H = \frac{P_{discharge} - P_{suction}}{\rho g} , \quad (2)$$

where H , Q , V and A denote pump head, flow rate, flow velocity, and cross-sectional area of the flow, respectively; ρ and g are flow density and gravitational acceleration, respectively. Further, one can evaluate static pressure and velocity changes for different values of flow rate and velocity.

Continuing with the research, three impellers of different outlet angles, namely 27°, 30°, and 33° were investigated at a rotation speed of 2000 rpm. As mentioned before, total pressure and velocity distributions and hence the pump head and efficiency values were then obtained at eight different flow rates. Presented here are the corresponding total pressure plots to a few flow rates only.

3.1. Total pressure contours

3.1.1. Outlet angle of 27°

Figs. 5 and 6 demonstrate total pressure contours corresponding to inlet velocities of 0.68 m/s (equivalent to a flow rate of 500 l/min) and 2.71 m/s (equivalent to a flow

rate of 2000 l/min), respectively.

3.1.2. Outlet angle of 30°

Figs. 7 and 8 demonstrate total pressure contours corresponding to inlet velocities of 2.03 m/s (equivalent to a flow rate of 1500 l/min) and 2.71 m/s (equivalent to a flow rate of 2000 l/min), respectively.

3.1.3. Outlet angle of 33°

Figs. 9 and 10 demonstrate total pressure contours corresponding to inlet velocities of 0.68 m/s (equivalent to a flow rate of 500 l/min) and 2.03 m/s (equivalent to a flow rate of 1500 l/min), respectively.

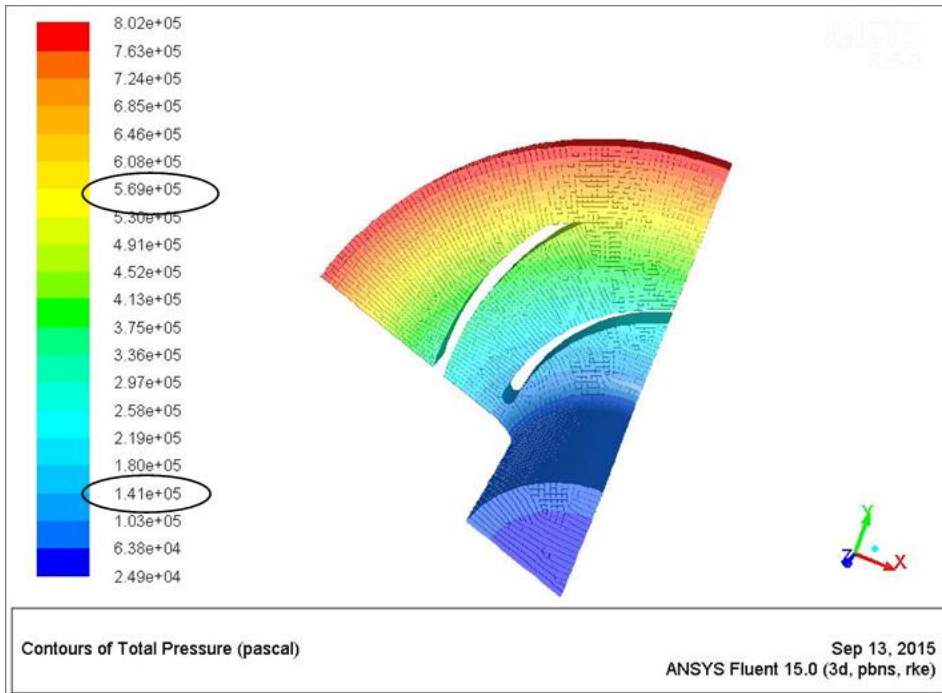


Fig. 5 Total pressure contours corresponding to the inlet velocity of 0.68 m/s; outlet angle: 27°

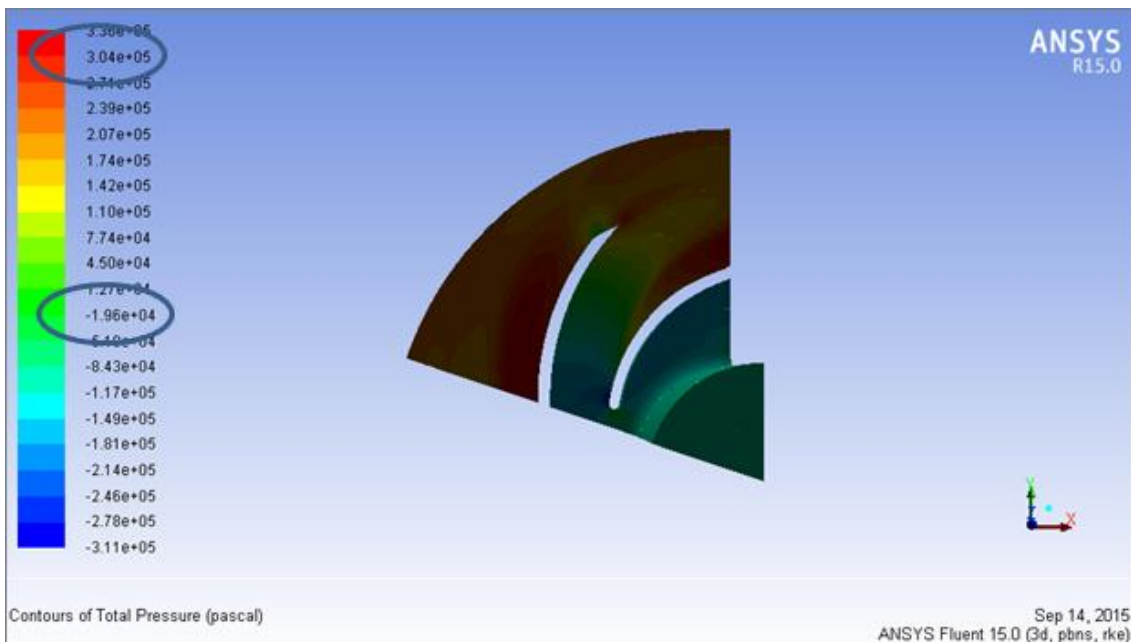


Fig. 6 Total pressure contours corresponding to the inlet velocity of 2.71 m/s; outlet angle: 27°

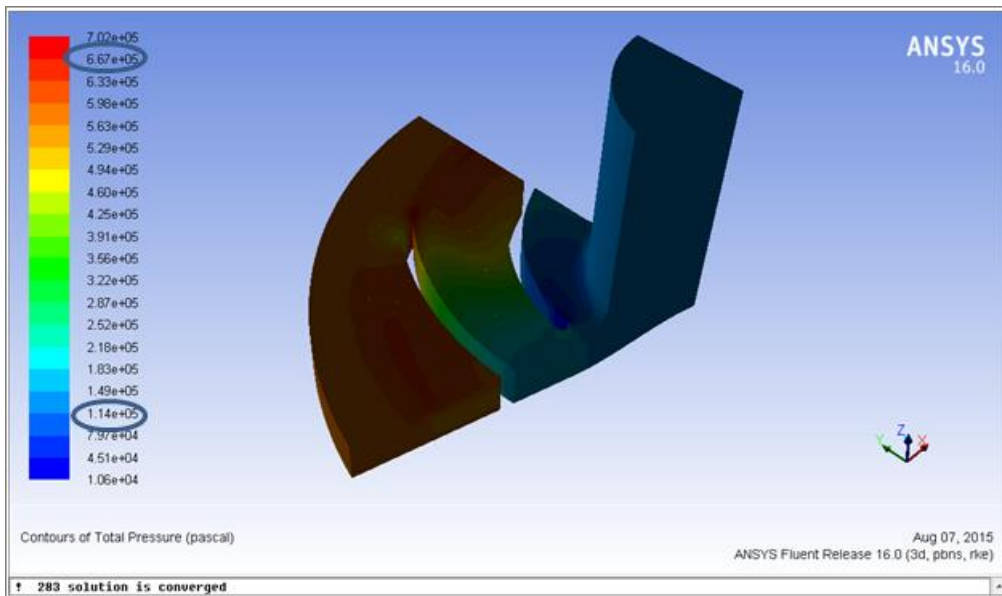


Fig. 7 Total pressure contours corresponding to the inlet velocity of 2.03 m/s; outlet angle: 30°

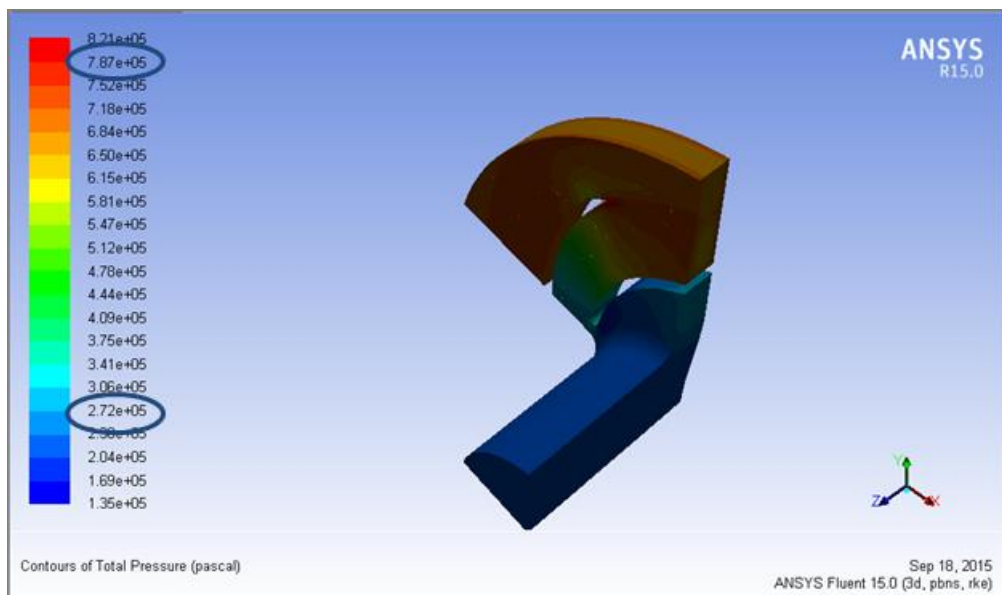


Fig. 8 Total pressure contours corresponding to the inlet velocity of 2.71 m/s; outlet angle: 30°

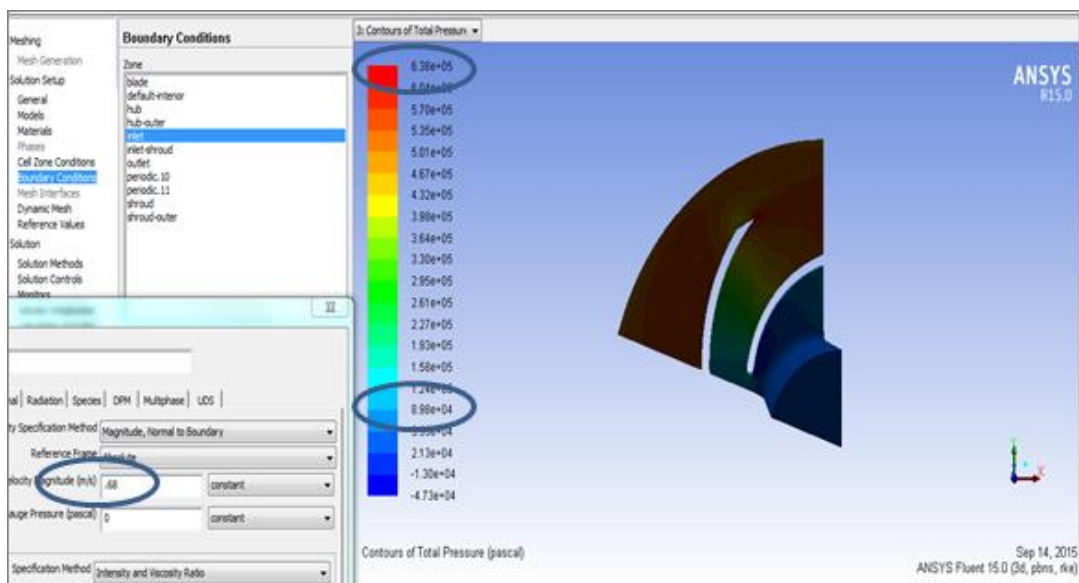


Fig. 9 Total pressure contours corresponding to the inlet velocity of 0.68 m/s; outlet angle: 33°

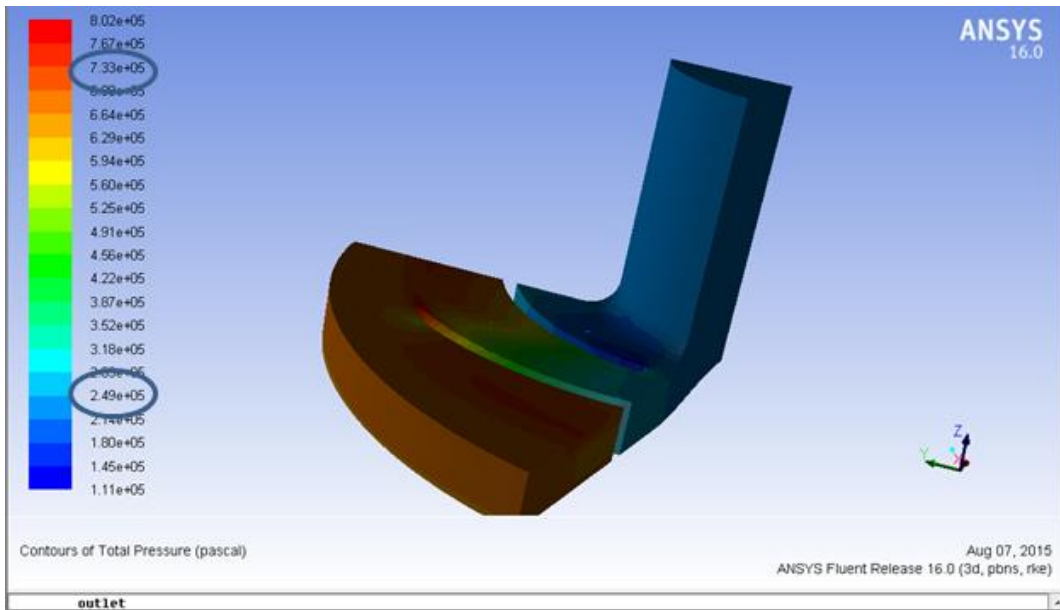


Fig. 10 Total pressure contours corresponding to the inlet velocity of 2.03 m/s; outlet angle: 33°

3.2. Head-flow rate performance curves

Using the pressure contours and Eq. (2), corresponding pump head values to different flow rates were

obtained. Where, pressure values are obtained from Fig. 7. Table 2 reports corresponding pump head values to eight different flow rates at each of the three outlet angles (27°, 30°, and 33°).

Table 2

Numerical values of pump head for eight different flow rates; outlet angles: 27°, 30°, and 33°

H, m			Q, lit/min
33 CFD	30 CFD	27 CFD	
54.8	58.5	42.8	500
53.8	57.8	41.8	1000
49.1	55.3	38.3	1500
40.2	51.4	32.4	2000
32.1	45.8	27.1	2500
22.6	36.7	17.6	3000
19.9	27.4	11.2	3230
12.7	19.8	6.9	3500

Plotted in Fig. 11 are the head-flow rate performance curves at each of the three outlet angles (27°, 30° and 33°). CFD analysis show that with the adjustment of H-Q

the impeller geometry of the pump, the head and efficiency at 30 degree outlet angle in comparison with other cases increase.

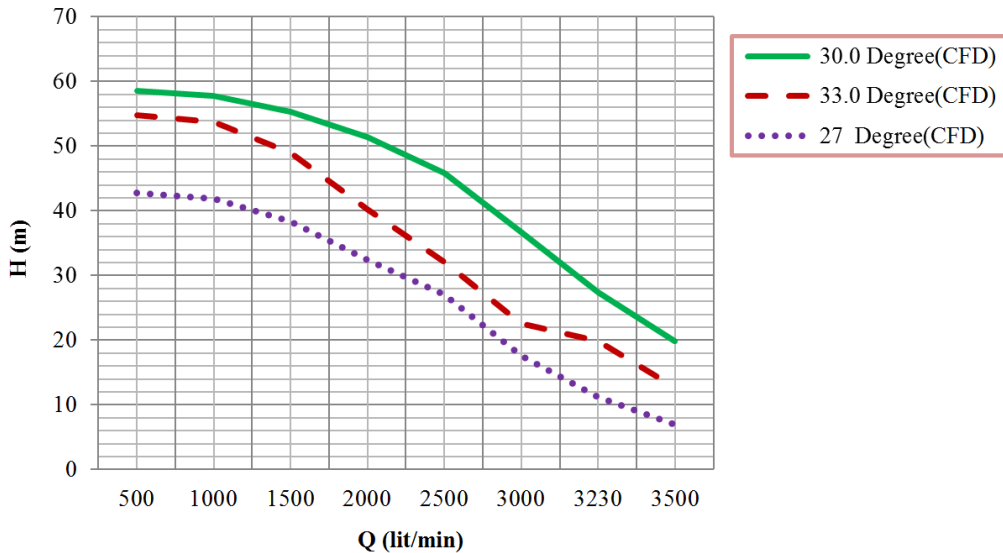


Fig. 11 Head-flow rate performance curves at each of the three outlet angles (27°, 30°, and 33°)

3.3. Efficiency-flow rate performance curves

Pump efficiency can be calculated from the Eq. (3):

$$\eta = \frac{\rho g H Q}{P}, \quad (3)$$

where, P denotes the pump input power (here 30 kW) and

η represents the pump efficiency. Reported in Table 3 are the values of efficiency in terms of flow rate for the three outlet angles.

Plotted in Fig. 12 is the efficiency-flow rate performance curves at each of the three outlet angles (27°, 30°, and 33°). CFD analysis show that the efficiency of pump in 2500 (lit/min) is maximum for all type of outlet angle blades and for 30 degree outlet angle is better than others.

Table 3

Numerical values of pump efficiency for eight different flow rates; outlet angles: 27°, 30°, and 33°

$\eta, \%$			$Q, \text{lit/min}$
33 CFD	30 CFD	27 CFD	
15.02	16.25	11.86	500
29.88	32.11	23.21	1000
40.83	40.08	31.91	1500
44.66	56.88	37.11	2000
45.61	63.61	37.51	2500
37.66	61.16	29.3	3000
35.71	49.16	20.02	3230
24.69	38.51	13.41	3500

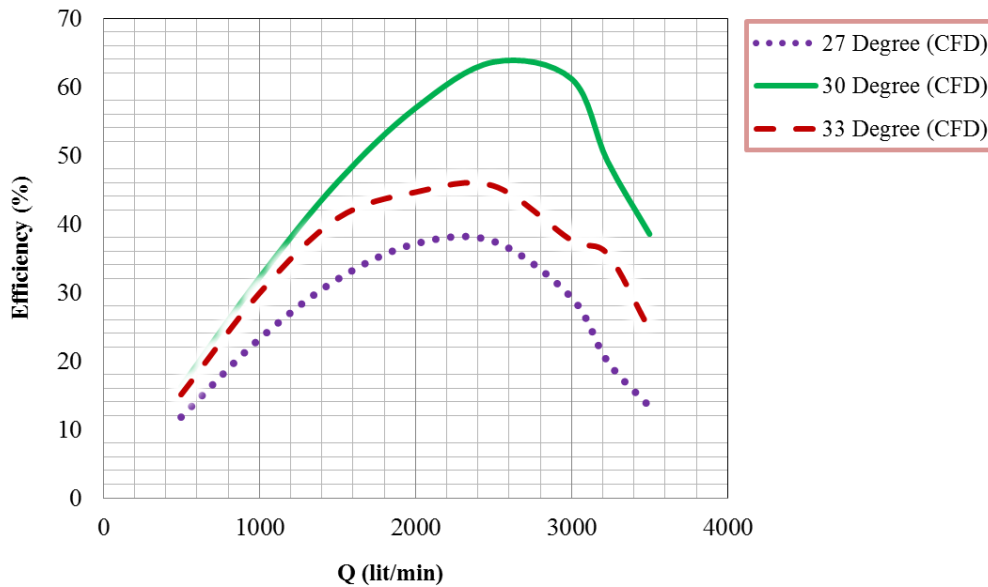


Fig. 12 Efficiency-flow rate performance curves at each of the three outlet angles (27°, 30°, and 33°)

4. Test

A multi-stage pump of 2000 rpm and 30 kW input power was used for the tests. The pump impeller was manufactured according to the specifications in Table 1. Figs. 13 and 14 demonstrate the used multi-stage pump and its impellers, respectively. For achieve the results of different outlet angle, initially according Fig. 13 disassemble a multi stage pump device and bring out the low pressure impeller from original shaft. After assembly the impeller with 27 degree outlet angle on the pump and install them on the chassis of midlum truck device. Then with set up the three parts of propeller shaft (one part fix and two part moveable) transfer the rotation of 2000 rapid per minute from motor to pump with power take off using the rapid meter for adjust the revolution that mounted on control panel. We start testing the pump in different flow rate

with opening the inlet valve that adjoined to water tank. At first install hose on the outlet then open the outlet valve and adjust the flow meter on 500 liter per minute. After start measure the head of the pump and note the results. Respectively repeat this for another flow rate (1000, 1500, 2000, 2500, 3000, 3500 lit/min). In the next step disclose pump from chassis and after disassemble, assembly the impeller with 30 degree outlet angle. Similar to first stage note the results the head of the pump in different flow rate. we will do all cycle for 33 degree outlet angle and note the outlet head and in next level compare these with CFD results.

Fig. 15 provides a schematic of test setup and testing machine. Pump suction the water from the tank and shooting the water then we can meter the head of pump in various outlet angle blade.



Fig. 13 The used multi-stage pump for the experimentations



Fig. 14 Pump impellers with different outlet angles: 27°, 30°, and 33°

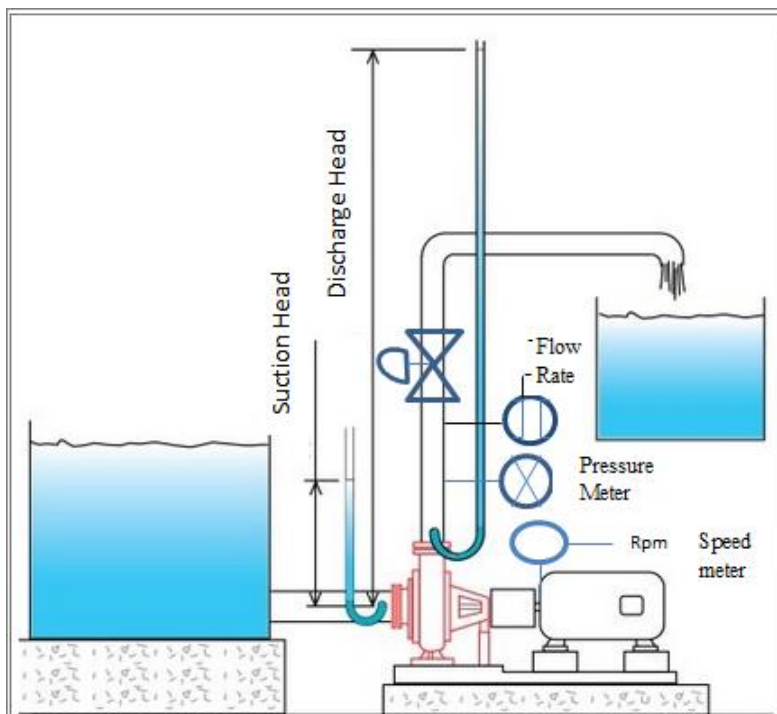


Fig. 15 The schematic of test setup

5. Experimental results

5.1. Head–flow rate performance curves

Table 4 reports corresponding experimental pump heads to eight different flow rates at each of the three outlet angles (27°, 30°, and 33°).

Plotted in Fig. 16 are the experimentally derived head-flow rate performance curves at each of the three outlet angles (27°, 30°, and 33°). The test show that with the adjustment of the impeller geometry of the pump, the head and efficiency at 30 degree outlet angle in comparison with other cases increases.

Table 4

Experimental values of pump head for eight different flow rates; outlet angles: 27°, 30°, and 33°

H, m			Q, lit/min
33 Exp	30 Exp	27 Exp	
53.2	55.1	40.3	500
52.5	54.5	38.8	1000
48.5	50.2	36.8	1500
42.8	45.5	31.9	2000
35.1	41.5	26.2	2500
25.8	29.8	20.1	3000
17.4	22.2	10.3	3230
12.2	15.1	5.3	3500

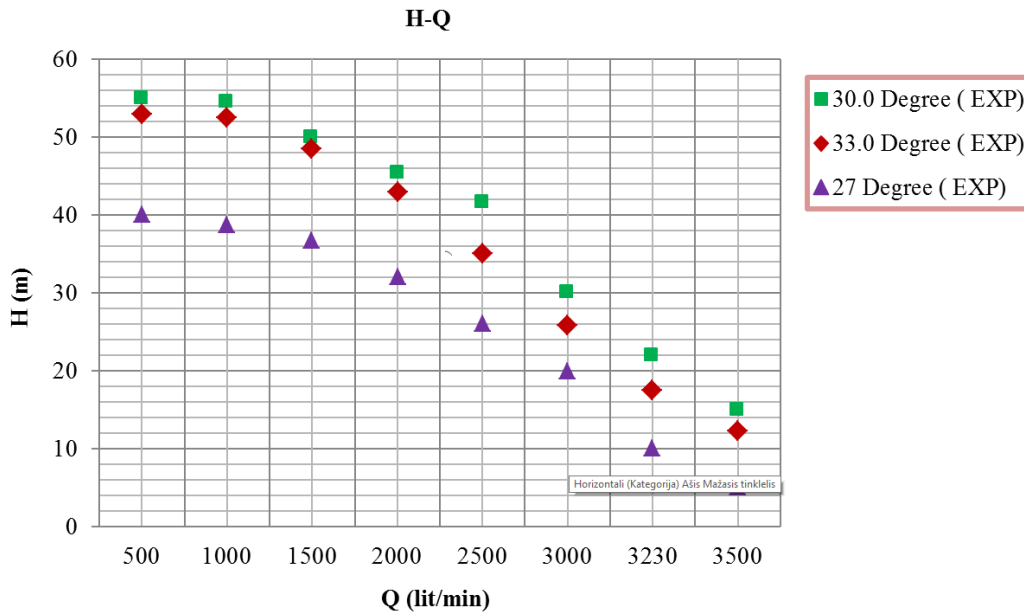


Fig. 16 Experimentally derived head-flow rate performance curves at each of the three outlet angles

5.2. Efficiency-flow rate performance curves

Table 5 reports corresponding experimental pump efficiencies to eight different flow rates at each of the three

outlet angles (27°, 30°, and 33°).

Plotted in Fig. 17 are the experimentally derived efficiency-flow rate performance curves at each of the three outlet angles (27°, 30°, and 33°).

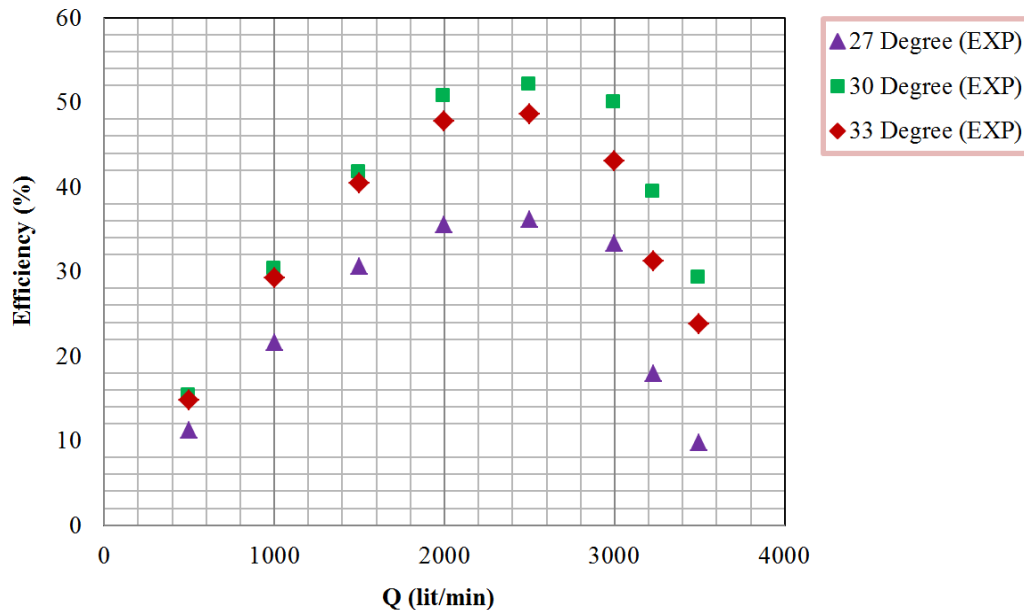


Fig. 17 Experimentally derived efficiency-flow rate performance curves at each of the three outlet angles

6. Simulation results versus experimental data and CFD model validation

Figs. 18 and 19 present the comparisons between the numerical and experimental results in terms of head-flow rate and efficiency-flow rate performance curves, respectively. The CFD analysis and experimental results

show that with the adjustment of the impeller geometry of the pump, the head and efficiency at 30 degree outlet angle in comparison with other cases increases and improves the centrifugal pump performance. Numerical and experimental results show that the efficiency of the pump in 2500 lit/min is maximum relative to the other cases.

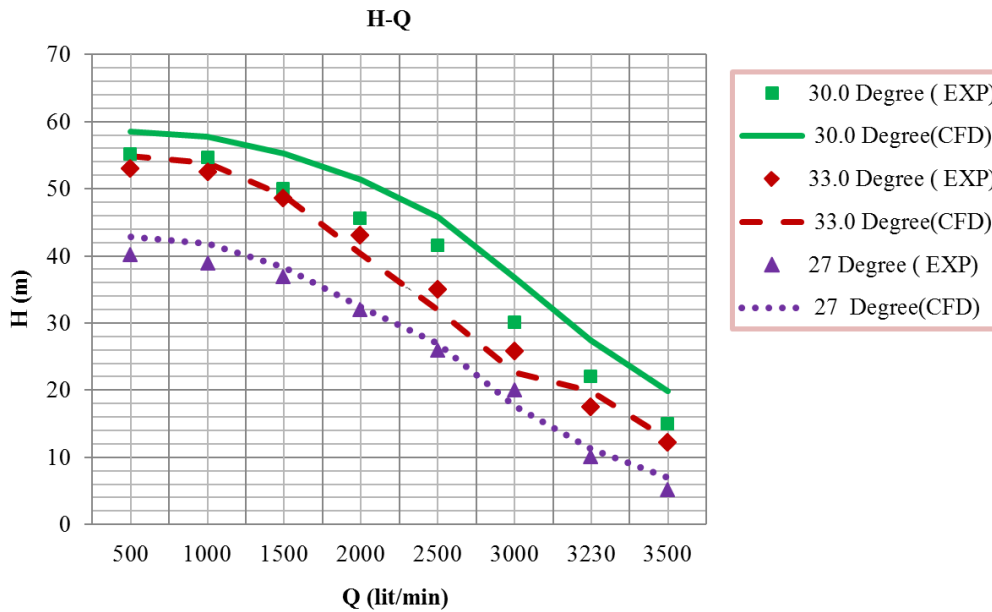


Fig. 18 Head-flow rate performance curve, outlet angles: 27°, 30°, and 33°

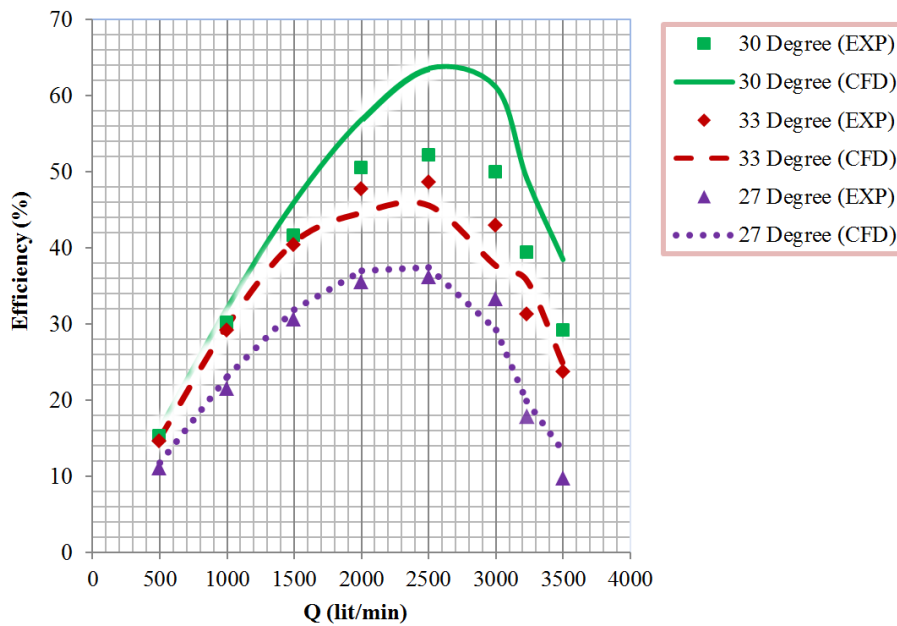


Fig. 19 Efficiency-flow rate performance curve, outlet angles: 27°, 30°, and 33°

Experimental values of pump efficiency for eight different flow rates; outlet angles: 27°, 30°, and 33°

Table 5

$\eta, \%$			$Q, \text{ lit/min}$
33 CFD	30 CFD	27 CFD	
14.72	15.27	11.11	500
29.16	30.27	21.55	1000
40.41	41.66	30.66	1500
47.77	50.55	35.55	2000
48.61	52.08	36.11	2500
42.87	50.12	33.33	3000
31.22	39.47	17.94	3230
23.72	29.16	9.77	3500

7. Conclusion

The effect of outlet angle geometry of multi-pressure pump impellers on the pump head and efficiency were investigated both numerically (via CFD) and experimentally. A closed single-suction, five-blade impeller was analyzed at three outlet angles: 27°, 30°, and 33°. First, the impeller model was developed in SOLIDWORKS software; then it was used to analyze the fluid flow using ANSYS Fluent software. Unstructured meshing approach was followed for all surfaces and volumes. Blade surfaces were meshed with square elements while quadrial elements were used to mesh the volumes. In the experimental part of the research, tested with three impellers of different outlet angles was a multi-stage pump of rotation speed and input power of 2000 rpm and 30 kW, respectively. Numerical simulation results were in good agreement with the test data, particularly at outlet angles of 27° and 33°. Therefore, one can save money and time by using numerical simulation tools provided by ANSYS Fluent, rather than undertaking experimental approaches.

Both numerical and experimental results indicated that, at specific values of outlet angle and blade width, hydraulic and mechanical losses within the impeller reduce, increasing the pump head and efficiency. Maximum pump head and efficiency were observed to occur at an outlet angle of 30°. This is because of the reduced losses due to water recirculation within the volute casing and outlet impellers. At this angle, improved energy transfer into the fluid (energy consumption) and better conductance of the flow by the main blades in the impeller outlet may result in increased pump head and efficiency.

Conflict of interests

The authors declare that there is no conflict of interests regarding the publication of this paper.

References

1. **Gulich, J.F.** 2010. *Centrifugal Pumps*, Springer-Verlag Berlin Heidelberg, Second edition, 966 p. <http://dx.doi.org/10.1007/978-3-642-12824-0>.
2. **Nourbakhsh, A.** 2005. *Turbo Machines*, Tehran university publications, Second edition.
3. **Stepanoff, A.J.** 1993. *Centrifugal and Axial Flow Pumps: Theory, Design and Application*, Krieger Publishing Company, Second edition, 470 p.
4. **Zhou, W.; Zhao, Z.; Lee, T.S.; Winoto, S.H.** 2003. Investigation of flow through centrifugal pump impellers using computational fluid dynamics, *International Journal of Rotating Machinery* 9(1): 49-61. <http://dx.doi.org/10.1155/S1023621X0300006X>.
5. **Hamkins, C.P.; Bross, S.** 2002. Use of surface flow visualization methods in centrifugal pump design, *Journal of Fluids Engineering* 124(2): 314-318. <http://dx.doi.org/10.1115/1.1470477>.
6. **Thin, K.C.; Khaing, M.M.; Aye, K.M.** 2008. Design and performance analysis of centrifugal pump, *World Academy of Science Engineering and Technology* 46: 422-429.
7. **Anagnostopoulos, S.** 2009. A Fast Numerical Method for Flow Analysis and Blade Design in Centrifugal Pump Impellers, *Computers & Fluids* 38(2): 284-289. <http://dx.doi.org/10.1016/j.compfluid.2008.02.010>.
8. **Grapsas, V.A.; Anagnostopoulos, J.S.; Papantonis, D.E.** 2005. Hydrodynamic design of radial flow pump impeller by surface parameterization, 1st International Conference on Experiments/Process System Modeling/Simulation/Optimization, Athens, 6-9 July.
9. **Kergourlay, G.; Younsi, M.; Bakir, F.; Rey, R.** 2007. Influence of splitter blades on the flow field of a centrifugal pump: test-analysis comparison, *International Journal of Rotating Machinery* 7: 1-13. <http://dx.doi.org/10.1155/2007/85024>.
10. **Bacharoudis, E.C.; Filoios, A.E.; Mentzos, M.D.; Margaris, D.P.** 2008. Parametric study of a centrifugal pump impeller by varying the outlet blade angle, *The Open Mechanical Engineering Journal* 2(1): 75-83. <http://dx.doi.org/10.2174/1874155X00802010075>.
11. **Houlin, L.; Yong, W.; Shouqi, Y.; Minggao, T.; Kai, W.** 2010. Effects of blade number on characteristics of centrifugal pumps, *Chinese Journal of Mechanical Engineering* 23(6).
12. **Tverdokhle, I.; Knyazeva, E.; Birukov, A.; Lugovaya, S.** 2010. About designing the flow part of a multi-stage pump with a minimum radial dimensions, *Procedia Engineering* 39: 84-90. <http://dx.doi.org/10.1016/j.proeng.2012.07.011>.
13. **Li, W.G.** 2013. Effect of flow rate and viscosity on slip factor of centrifugal pump handling viscous oils, *International Journal of Rotating Machinery* Article ID 317473. <http://dx.doi.org/10.1155/2013/317473>.
14. **Zhou, X.; Zhang, Y.; Ji, Z.; Hou, H.** 2014. The optimal hydraulic design of centrifugal impeller using genetic algorithm with BVF, *International Journal of Rotating Machinery* Article ID 845302. <http://dx.doi.org/10.1155/2014/845302>.
15. **Bellary, S.A.L.; Samad, A.** 2014. Improvement of efficiency by design optimization of a centrifugal pump impeller, *ASME*. <http://dx.doi.org/10.1115/gt2014-25217>.
16. **Zhang, Q.; Zhou, H.; Gao, Q.; Cui, Z.** 2014. Analysis of effects of impeller inlet width on the performance of centrifugal pump, *Journal of Chemical and Pharmaceutical Research* 6(5): 2078-2081.

N. Mohammadi, M.Fakharzadeh

ANALYSIS OF EFFECT OF IMPELLER GEOMETRY INCLUDING BLADE OUTLET ANGLE ON THE PERFORMANCE OF MULTI-PRESSURE PUMPS: SIMULATION AND EXPERIMENT

S u m m a r y

In this paper, the effect of outlet angle geometry of the blades of the impeller of a multi-pressure pump on the pump's head and efficiency using two approaches, namely numerical approach (Computational Fluid Dynamics) and experimentation are investigated. Herein, a closed single-suction, five-blade impeller with three different outlet angles (27°, 30°, and 33°) is analyzed. The impeller model was first built in SOLIDWORKS software before analyzing the fluid flow with the help of ANSYS Fluent software. All surfaces were meshed through irregular grid-

ding. Considering high flow velocity along with low thickness of boundary layer near the blade tips, smaller mesh sizes were used across these areas. Blade surfaces were meshed using square elements. Furthermore, in order to model the volumes, irregular gridding and TGrid algorithm were undertaken. Generated with this algorithm are quadrial elements of known size. In volumetric meshing stage, aspect ratio was set to a maximum of 0.6. In the experimentation phase of this research, a multi-stage pump was tested at 2000 rpm and 30 kW of input power with three impellers of different angles. At specific values of outlet angle and impeller outlet width, some reductions in hydraulic and mechanical losses within the impeller along with some rises in the pump head and efficiency were observed. Simulation results were found to be in good

agreement with the experimental data; so as one can save time and money by using numerical simulation approaches in ANSYS Fluent rather than undertaking experimentations. Numerical and experimental analyses revealed that the maximum pump head and efficiency have been witnessed at the outlet angle of 30°. This is because of the reduced losses by water recirculation within the volute and outlet impellers.

Keywords: Impeller Geometry, centrifugal pump, ANSYS Fluent.

Received October 05, 2016

Accepted February 06, 2017